ARCHIVES of FOUNDRY ENGINEERING

ISSN (2299-2944)
Volume 2024
Issue 2/2024

88 – 97

10/2

10.24425/afe.2024.149274

Published quarterly as the organ of the Foundry Commission of the Polish Academy of Sciences

Synthesis and Characterization of Novel Aluminum Composites: A Compo-Casting Approach with ZrO_2, Al_2O_3, and SiC

S. Farahany [a, *], M.K. Hamdani [b], M.R. Salehloo [b], M. Krol [c], E. Cheraghali [a]

[a] Buein Zahra Technical University, Iran
[b] Iran University of Science and Technology, Iran
[c] Silesian University of Technology
* Corresponding author: E-mail address: farahany@bzte.ac.ir

Received 11.01.2024; accepted in revised form 18.04.2024; available online 05.06.2024

Abstract

The present study evaluates the microstructural features, mechanical properties, and wear characteristics of the newly developed hybrid composite of A356/ZrO_2/Al_2O_3/SiC produced by compo-casting at 605±5 °C, 600 rpm for 15 minutes with less than 30% solid fraction in which Bi and Sn were added separately to the matrix before introducing reinforcements. FESEM micrographs and corresponding EDS illustrated the successful incorporation of particles in the matrix. Fine particles of ZrO_2 were observed close to the coarse Al_2O_3, and SiC particles, along with Bi and Sn elements, were detected at the eutectic evolution region. The A356+Bi/Al_2O_3+ZrO_2+SiC hybrid composite exhibited the lowest specific wear rate (1.642×10^{-7} cm^3/Nm) and friction coefficient (0.31) under applied loads of 5, 10, and 20 N, in line with the highest hardness (73.4 HBN). Analysis of the worn surfaces revealed that the wear mechanism is mostly adhesive in all synthesized composites, which changed to the combination of adhesive and abrasive mode in the case containing Bi and SiC. Inserting Bi not only leads to the refinement of eutectic Si but also enhances the adhesion between the matrix/particles and improves lubricity. This, in turn, reduces the wear rate and coefficient of friction, ultimately improving the performance of the hybrid composite.

Keywords: Hybrid composite, Aluminum, Compo-casting, Wear, Bismuth

1. Introduction

Aluminium Metal Matrix Composites (AMMCs) have received much attention because of their unique combination of low density, good corrosion resistance, heat treatability, and excellent mechanical properties. Adding reinforcing particles such as SiC, B_4C, TiC, Al_2O_3, ZrO_2, TiO_2, and TiB_2 has improved aluminum composites' mechanical and tribological properties [1–3]. According to the industry requirements, production costs, and material availability, a single reinforcing particle may not impart the necessary properties for specific applications in aluminum composite materials. Therefore, scientists turned to the simultaneous use of two or more different reinforcements with various shapes and sizes, so hybrid metal matrix composites (HMMCs), known as the second generation of composites, have been introduced [4] to achieve unique properties [5–7]. Hybrid composites provide increased flexibility and dependability when designing potential components based on the combination and composition of the reinforcing particles [8]. Increased strength-to-weight ratio, improved hardness, toughness, and wear resistance compared to single-reinforced composites, indicating that aluminum hybrid metal matrix composites (AHMMCs) could be utilized in the design of components for automobile (e.g., pistons,

brake plates, and drums, connecting rods, engine, cylinder, crankshaft, bearings, sprockets, and pulleys), aircraft (e.g., wings, airplane chassis, and fuselage), building and construction (e.g., bridge decks, fall protection, and as a shield against the sunlight for buildings, window frames, door panels, and roof structures), marine (e.g., fast-moving boats), sport and recreations, rail transport, and defense [8–12].

James *et al.* [11] fabricated a hybrid composite with 6061 matrix alloy, 5% of ZrO_2, and 5% of Al_2O_3 and reported significant improvement in mechanical properties. According to Pranavi *et al.* [13], an increase in B_4C and Al_2O_3 ceramic particles within the 5059/B_4C/Al_2O_3 hybrid composite was correlated with the enhancement of tensile strength and hardness. Conversely, elongation values are negatively associated with the concentration of B_4C and Al_2O_3 particles. Rajmohan *et al.* [6] have indicated that the Al/10SiC-3mica hybrid composite exhibits superior strength, hardness, and wear resistance. It has been reported that adding the B_4C particles enhanced the wear properties of the AA6351-SiC composite [14].

The stir-casting method has received more attention due to its commercial viability, flexibility, and simplicity. However, this method faces drawbacks such as inadequate wettability, uneven distribution of reinforcement, porosity, clustering, and segregation [15]. Therefore, the reinforcement particles can settle at the bottom of the crucible, float on the surface, and agglomerate due to the high surface tension of the molten metal. Thus, a reduction in mechanical properties is a commonly anticipated outcome. Various techniques such as compo-casting, pre-heating, coating of particles, and ultrasonic, electromagnetic, and alloying agent addition have been performed to improve the metal-reinforcement wettability [16]. The compo-casting route is a superior method that can enhance the wetting between the molten matrix alloy and the reinforcements and facilitate uniform dispersion of the reinforcement particles within the solidified matrix [17].

Mg [18,19], Sr [20], Ti [21,22], Cu [23], Zr [22], and Cr [24] have been added to the molten matrix to enhance wettability. Low-melting point elements such as Bi, Sn, Pb, and Cd are free-machining elements and improve the machinability of Al alloys [25]. It has been reported that Bi can improve the tribological properties [26,27] and machinability [28,29] of aluminum alloys. The use of lubricating materials incorporating metal matrix composites is rising due to the growing demand for environmentally friendly or sustainable tribology and enhanced energy efficiency. Graphite has been added to the Al matrix to fabricate a self-lubricating composite. Nevertheless, the addition of graphite particles reduces the mechanical properties of AA6351[30] and AA6082 alloy [31], so it is used less in engineering applications. A similar deteriorative effect of graphite on mechanical properties has been reported for AA7050/B4C/Gr hybrid composite [32].

Based on the literature review, no comprehensive analysis has been carried out in fabricating hybrid aluminum matrix composites through compo-casting containing Bi and Sn and their properties. Combining reinforcing particles and alloying agents in composite materials can produce favorable and adverse effects. While these constituents may improve the material's properties, they can initiate unintended interactions that compromise functionality. Therefore, thoroughly investigating the effects of such particles in hybrid composites is crucial. This study aims to analyze the impact of Bi and Sn Bi addition on the microstructure, mechanical, and wear properties of hybrid composites containing Al_2O_3, ZrO_2, and SiC reinforcing particles.

2. Experimental Procedure

A 1kg alloy (Al-7Si-0.4Mg) ingot, which is of great interest, was selected for the matrix alloy. The matrix alloy was placed in a SiC crucible and melted using an electrical furnace. Subsequently, the temperature was maintained at 605±5 °C to achieve a semi-solid state, and mechanical stirring was applied using a single-stage impeller. A weighted Al_2O_3 (particle size of 250±60 μm), ZrO_2 (particle size of 10±5 μm), and SiC (particle size of 150±30 μm) were pre-heated at 300 °C for 20 min. Then, each reinforcing particle was slowly added to the stirred vortex melt .The particles were introduced to the melt in 3 steps with a time interval of 5 minutes at 600 rpm rotation speed. Mechanical stirring was carried out at 605±5 °C, speed of 600 rpm for 15 min. A k-type thermocouple controlled the temperature during stirring. Before pouring the melt into the permanent steel mold (50 mm height, 30 mm inert diameter), the melt temperature was increased to 700 °C and stirred manually for 1 min. When it was necessary to add Bi and Sn, these elements were added to the melt before adding reinforcing particles and stirring. Details of synthesized composites were tabulated in Table 1.

Table 1.
Chemical composition of synthesized hybrid composites (wt.%).

Sample No.	Si	Mg	Al_2O_3	ZrO_2	SiC	Sn	Bi
1	7.02	0.40	2.5	2.5	-	-	
2	7.24	0.35	2.5	2.5	-	-	0.5
3	7.09	0.41	2.5	2.5	-	0.5	-
4	7.10	0.40	1.6	1.6	1.6	-	0.5

The casting samples (Fig.1a) were cut longitudinally to analyze the microstructure (Fig.1b). After sanding, polishing, and etching, the samples were evaluated under a field emission scanning electron microscope (TESCAN MIRA3) with energy-dispersive X-ray (EDS). Dry sliding wear is conducted on Pin-on-Disc wear testing according to ASTM- G99 standard. The test was performed under a load of 5, 10, and 20N, a sliding speed of 0.2 m/s, and a sliding distance of 1000 m (Fig.1c and Fig.1d) at ambient temperature. A steel with 230 HBN hardness was chosen as a disk counterpart. After running continuously, the specimens were removed and cleaned with acetone, and the weight loss was measured.

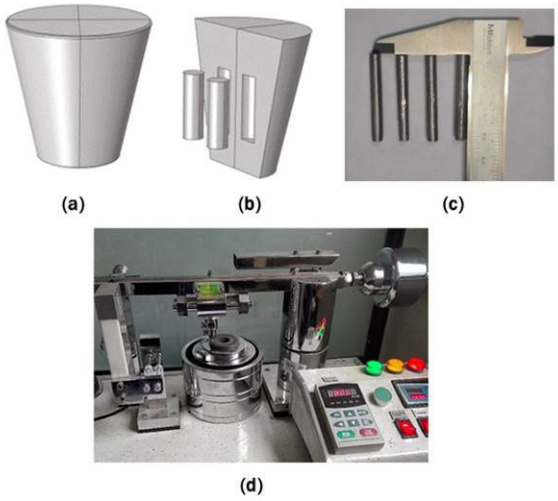

Fig. 1. Schematic illustration of (a) cast composites, (b) longitudinally cut for microstructural analysis and pin preparation, (c) machined pins, and (d) wear test apparatus

The wear test was repeated two times for each condition, and the mean value was reported. The specific wear rate (SWR) was calculated by using equation (1) as follows:

$$SWR = \frac{\Delta W}{\rho \times F \times D} \ (cm^3/N.m) \quad (1)$$

Where ΔW is the weight loss in g, ρ is the specimen's density g/cm^3, F is the normal load in N, and D is the sliding distance in m. Finally, the worn surfaces were examined in detail through FESEM to explore the wear mechanism. The hardness of the composites was measured by a Brinell hardness tester (Koopa - UV3) with a load of 62.5 kg and a tip diameter of 2.5 mm. The reported results are the mean value calculated from five measurements taken from distinct regions for each sample.

3. Results

3.1. Microstructure analysis

Fig. 2a displays the microstructure of sample 1, comprised of Al_2O_3 and ZrO_2 reinforcements. The primary Al and eutectic Al-Si phases, the dominant phases of the A356 alloy, are visible, along with the embedded particles in the eutectic Al-Si regions, where the final solidification occurs. The solidification front pushes the suspended particles towards the areas of the freezing end due to particle-pushing phenomena. Further observation of Fig.2a revealed the sign of discontinuity at the particle/matrix interface and agglomeration of finer particles. This phenomenon can be related to the lack of wetting of particles by the molten aluminum and their inherent tendency to attract each other due to electromagnetic forces. The particle/matrix interface of the hybrid composite was evaluated at higher magnification (Fig. 2b). The corresponding EDS analyses of the particles were displayed in Fig. 3, wherein the point A and point B particles were identified as Al_2O_3 and ZrO_2, respectively. It is worth noting that ZrO_2 particles could be observed within the eutectic region and close to Al_2O_3 particles.

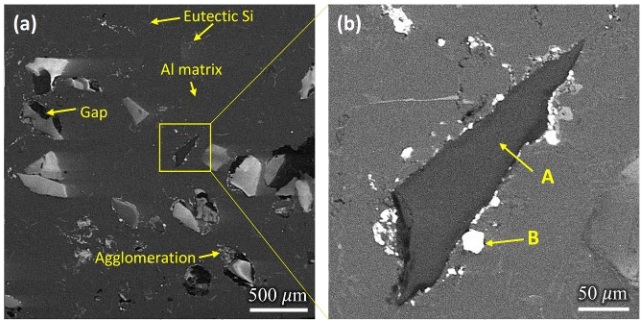

Fig. 2. (a) SEM micrograph of A356/Al_2O_3+ZrO_2 hybrid composites and (b) Al_2O_3+ZrO_2/ matrix interface

Fig. 4a illustrates the microstructure of sample 2, wherein the A356 matrix alloy was treated with Bi before incorporating Al_2O_3 and ZrO_2 particles. EDS analyses (Fig. 4b) of these more glowing particles, marked as C, confirmed the composition as Bi elements. Strikingly, Bi was found surrounding the Al_2O_3 particles. These observations corresponded to the findings previously reported regarding Bi particles near the reinforcements [27].

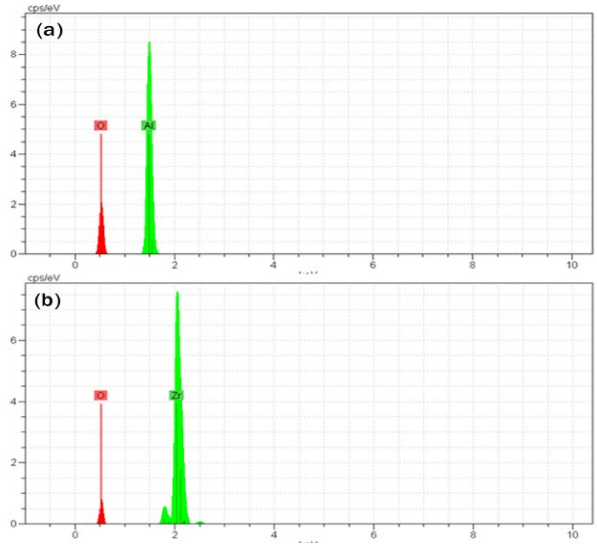

Fig. 3. EDS spectra of (a) point A and (b) point B in Fig. 2b

On the other hand, adding Bi is expected to reduce aluminum's surface tension, enhancing wetting behavior [33]. As a result, the particles were better covered by the matrix, with fewer instances of discontinuity observed at the particle/matrix interface. Furthermore, this factor assists in achieving a more uniform distribution of particles with different densities and physical properties.

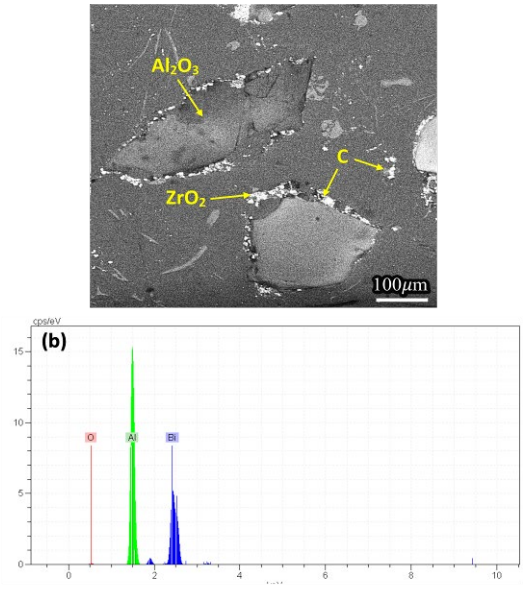

Fig. 4. (a) SEM micrograph of A356+Bi/Al_2O_3+ZrO_2 hybrid composites. (b) EDX spectrum of point C

Fig. 5 presents the microstructure of the A356/Al_2O_3+ZrO_2 hybrid composite containing the Sn element. The incorporation of Al_2O_3 and ZrO_2 into the matrix is apparent, with numerous bright particles spread adjacent to the particles.

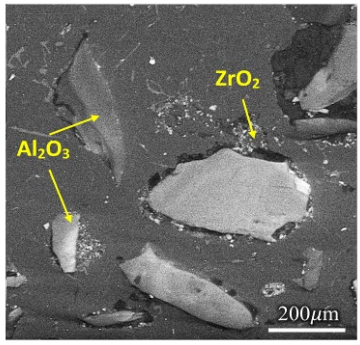

Fig. 5. SEM micrograph of A356+Sn/Al_2O_3+ZrO_2 hybrid composites

Upon closer inspection of the bright particle (marked D) through higher magnification (Fig. 6a), its composition was verified through EDS analysis (Fig. 6b), confirming that Sn elements were predominantly distributed near the eutectic Si area. Fewer ZrO_2 particles can be observed around the Al_2O_3 in the A356+Sn/Al_2O_3+ZrO_2 hybrid composite. In addition, a non-uniform distribution of ZrO_2 particles around the Al_2O_3 can be seen. The effect of adding Sn seems less than that of Bi addition. However, more studies are needed to shed more light on this issue. It may be related to the formation of Sn-Al-Si compounds during the hybrid composite's solidification process, which reduces the role of the Sn element.

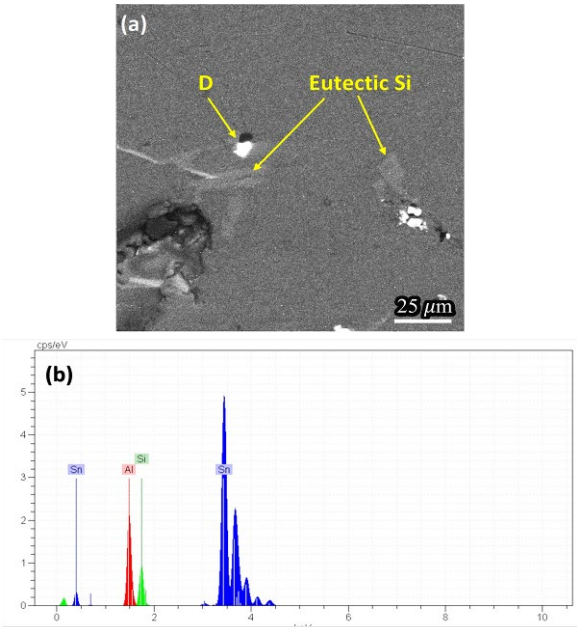

Fig. 6. (a) SEM micrograph of the bright particle in the A356+Sn/Al_2O_3+ZrO_2 hybrid composites and (b) EDX spectrum of point D

Fig. 7 presents the microstructure of a hybrid composite comprising Al_2O_3, ZrO_2, and SiC particles with Bi. It can be seen that all reinforcement particles are embedded within the matrix. Like Mg, Bi can enhance the wetting of particles by increasing solid surface energy, reducing molten surface tension, or decreasing the interfacial energy between the molten and solid phases [33]. Fig. 8 displays all visible phases' corresponding EDS spectra. Figs. 8a-8d confirm the presence of SiC particles (marked A), Bi (marked B), ZrO_2 (marked C), and Al_2O_3 (marked D), respectively.

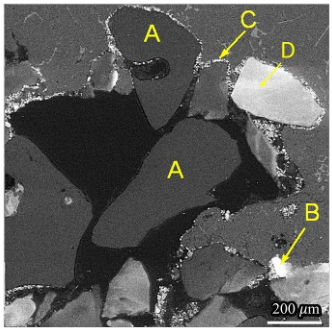

Fig. 7. SEM micrograph of A356+Bi/Al_2O_3+ZrO_2+SiC hybrid composites

3.2. Hardness

Fig. 9 illustrates the hardness variations of the synthesized composites. It has been reported that incorporating Al_2O_3, ZrO_2, and SiC particles into the A356 alloy enhanced the composite's hardness [34]. The hardness of the A356/Al_2O_3+ZrO_2 composite

was around 65.1 HBN, which increased to 71.2 HBN after adding Bi.

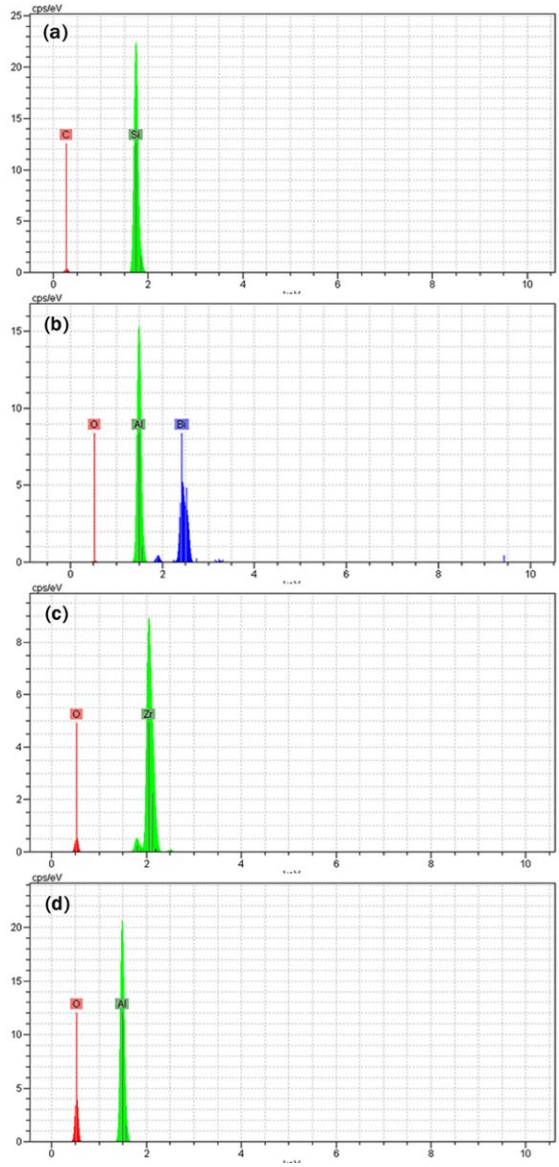

Fig. 8. EDX spectra of marked phases in Al_2O_3+ZrO_2+SiC+Bi hybrid composites in Fig.7: (a) SiC, (b) Bi, (c) ZrO_2, and (d) Al_2O_3

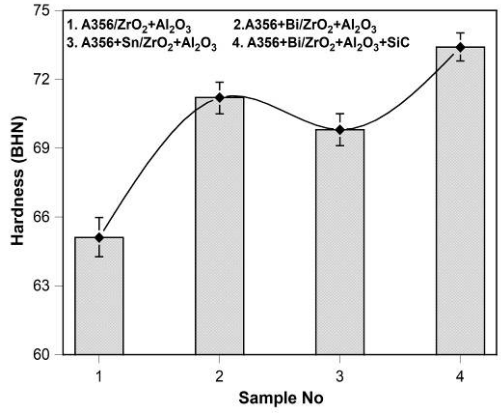

Fig. 9. Hardness values of hybrid composites: (1) A356/ Al_2O_3+ZrO_2, (2) A356+Bi/ Al_2O_3+ZrO_2, (3) A356+Sn/ Al_2O_3+ZrO_2 and (4) A356+Bi/ Al_2O_3+ZrO_2+SiC

This may be because Al_2O_3 and ZrO_2 obstruct the dislocation motion, increasing the hardness. It has been shown that the hardness of 7075 alloy improved by reinforcing the matrix with multiple SiC and B_4C reinforcements [35]. It is important to note that adding Bi can induce the refinement of coarse eutectic Si in hypo-eutectic Al-Si [33], improving hardness. However, the hardness of the A356/Al_2O_3+ZrO_2 composite decreased slightly to 69.8 HBN after adding the Sn element. Finally, the hardness of the A356+Bi/ Al_2O_3+ZrO_2+SiC hybrid was measured at 73.4 HBN. Adding SiC with higher hardness increases the hardness of the hybrid composite [36] to the highest value. It has been shown that the 5083/SiC/CeO_2 hybrid composite is 40% harder than the 5083 base metal [37]. Numerous factors affect the hardness of aluminum composites, including particle size and distribution, matrix-reinforcement bonding strength, the matrix's chemical composition, type, quantity of reinforcing phase, processing conditions, and heat treatment methods. The selection of the reinforcing material can dramatically impact the composite's hardness, with materials possessing greater rigidity relative to the matrix, leading to an overall increase in the hardness. However, the interfacial bonding strength plays a significant role in determining the composite's hardness.

3.3. Wear characteristics

The wear behavior of composites is a significant factor in determining their suitability, durability, maintenance cost, and overall performance in various applications. The wear characteristics were assessed based on specific wear rate (SWR) and friction coefficient (FOC) measurements from pin-on-disc tribological tests, and the mean values were reported. Fig.10 depicts the specific wear rate alterations for the fabricated composites under 5, 10, and 20N applied loads. Wear is predominantly a surface phenomenon, with the reinforcements experiencing localized force impacts. Accordingly, the distribution of the reinforcements is of particular significance. The SWR increased with the increase in the applied load from 5

to 20N, which is in accordance with Dinaharan et al. [38]. It can be seen that the SWR of composites containing Bi and Sn is lower than that of those without Bi and Sn under different loads. For the applied load 5N, the highest wear rate of 2.537 $\times 10^{-7}$ cm^3/Nm was obtained for the A356/ZrO_2+Al_2O_3 hybrid composite. The wear rate decreased to 1.94 $\times 10^{-7}$ cm^3/Nm after adding Bi and then shifted to 2.223$\times 10^{-7}$ cm^3/Nm after adding Sn. The lowest wear rate was measured at 1.642 $\times 10^{-7}$ cm^3/Nm for A356+Bi/ZrO_2+Al_2O_3+SiC hybrid composite. Adding Bi and Sn helps reduce the metal-to-metal interaction between the pin and disc, decreasing the wear rate. For the 10N load, the SWR was measured at 5.770 $\times 10^{-7}$ cm^3/Nm for A356/ZrO_2+Al_2O_3, which fell to 3.921 $\times 10^{-7}$ cm^3/Nm after adding Bi. The SWR increased to 4.422$\times 10^{-7}$ cm^3/Nm for composite containing Sn. After inserting SiC into the A356+Bi/ZrO_2+Al_2O_3 hybrid composite, the SWR decreased to the lowest value of 3.421$\times 10^{-7}$ cm^3/Nm. The SWR increased significantly after an increase of applied load up to 20N. It reached the highest value of 14.642×10-7 cm^3/Nm for A356/ZrO_2+Al_2O_3 hybrid composite. The SWR decreased sharply to 11.920$\times 10^{-7}$ cm^3/Nm for A356+Bi/ZrO_2+Al_2O_3 hybrid composite for 20N applied load.

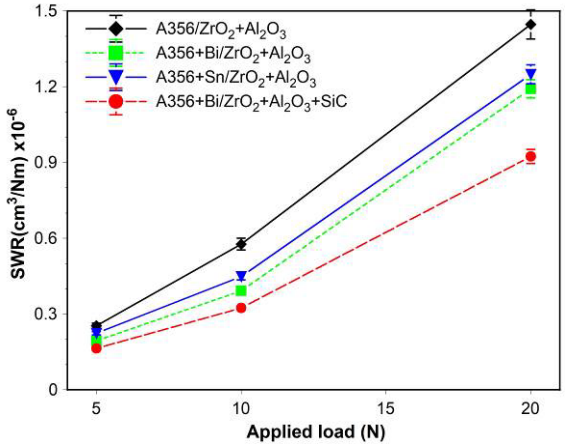

Fig. 10. Variations of specific wear rate as a function of applied load for fabricated hybrid composites

Adding Sn increased the SWR to 12.490$\times 10^{-7}$ cm^3/Nm compared to the Bi addition. Moreover, the lower SWR (9.242$\times 10^{-7}$ cm^3/Nm) was obtained for A356+Bi/ZrO_2+Al_2O_3+SiC hybrid composite. The wear rate is closely related to the type of reinforcement material and the bonding features between the reinforcements and matrix. Improve bonding adhesion of hybrid composites due to adding Bi or Sn leads to a lower wear rate.

On the other hand, despite the low hardness, Bi and Sn act as solid lubricants and mitigate wear rates. Particles operate as a protective barrier against extreme destructive action caused by the counter face. This is attributed to the strong interface bond, a crucial factor in transferring loads from the matrix to the hard particles, consequently reducing material wear [14]. So, the wear rate of Al_2O_3+ZrO_2+SiC+Bi is lower than Al_2O_3+ZrO_2+Bi due to adding more rigid SiC particles. Fig.11a illustrates the frictional coefficient graph as a function of sliding distance for various hybrid composites, all subjected to a 5N applied load.

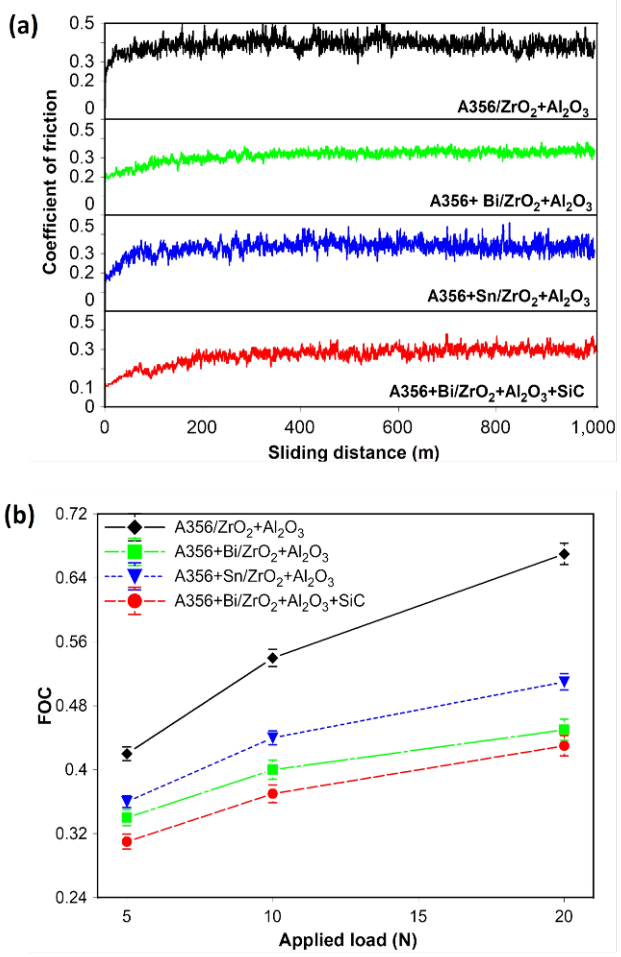

Fig. 11. (a) Friction of coefficient vs. sliding distance for different hybrid composites under 5N applied load. (b) Variations of coefficient friction as a function of applied loads for fabricated hybrid composites

The chart can determine the frictional behavior of the surfaces in contact. During the wear test, the friction coefficient for the A356/ZrO_2+Al_2O_3 composite experiences an initial rise, followed by a gradual ascent to reach a stable level, which persists after a sliding distance of 100 m. This initial increase, followed by the stabilization of the friction coefficient, occurred after sliding of 250 m for the A356+Bi/ZrO_2+Al_2O_3 composite. For the A356+Sn/ZrO_2+Al_2O_3 composite, a shorter sliding distance (150 m) is needed to achieve a consistent and stable friction coefficient. Furthermore, for the A356+Bi/ZrO_2+Al_2O_3+SiC composite, a longer sliding length of 300 m was required to attain a constant friction coefficient value. The average FOC of the A356/ZrO_2+Al_2O_3 composite is around 0.42, dropped to 0.32 after adding Bi to the A356/ZrO_2+Al_2O_3 composite.

Additionally, the FOC of A356+Sn/ZrO_2+Al_2O_3 is around 0.36, which decreased to 0.31 after inserting SiC particles into A356+Bi/ZrO_2+Al_2O_3. Fig. 11b displays the FOC values for various hybrid composites under 5, 10, and 20 N applied loads. The average FOC of all hybrid composites under 20 N applied

load is greater than that for the 10 N and 5 N. It is generally accepted that FOC increases with increasing the applied load.

However, the A356/ZrO_2+Al_2O_3 composites rise faster than other fabricated composites. It can be seen that the FOC decreased after adding Bi and Sn into the A356/ZrO_2+Al_2O_3 composites. This trend aligns with the friction coefficient findings reported by Riahi et al. [39] in their study of the Al-SiC hybrid composite containing graphite. However, the role of Bi in reducing the FOC is more significant than adding Sn at three loads of 5 N, 10 N, and 20 N. For example, at an applied load of 10N, the reduction after adding Bi and Sn was 26 % and 18%, respectively. This percent reduction in friction coefficient was 32% and 23% for 20 N load, suggesting that the lubricating role of Bi and Sn becomes more prominent under higher applied loads. This may be due to increased friction and heat generation at the contact surfaces.

The reduction in friction for A356+Bi/ZrO_2+Al_2O_3 and A356+Sn/ZrO_2+Al_2O_3 composites compared to the A356/ZrO_2+Al_2O_3 composite can be mainly related to the gradually release Bi and Sn lubricating elements onto the worn surface, thereby diminishing shear stress. However, the effect of Bi is more colorful than Sn in lubricant conditions.

Additional investigation is needed to illuminate this matter further. According to Archard's law [40], a direct relationship exists between composite materials' hardness and wear resistance. As the composite's hardness increases, its wear rate decreases, indicating higher wear resistance. However, recent research suggests this rule may not apply to all synthesized composites. For example, the hardness was lower in certain composite materials containing three reinforcing particles and an Sn element than in other tested composites. Harder particles (SiC), alongside ZrO_2 and Al_2O_3 particles, appear to have mitigated the negative impact of lower bonding strength between the matrix and reinforcement components on the composite's properties.

3.4. Worn surfaces

The worn surfaces of hybrid composites were analyzed using FESEM to gain insights into the wear mechanisms. Fig. 12 illustrates the FESEM micrographs of the worn surfaces of the produced hybrid composites, tested at loads of 5 N. Fig. 12a and 12b illustrate the worn surface of the A356/Al_2O_3+ZrO_2 composite, with delamination of the sample surface observed, suggesting the adhesive is the primary wear mechanism. The EDS of Zone 1 and Zone 2, shown in Fig.13a and Fig.13b, respectively, exhibit the presence of O, Al, Si, and Fe, confirming that the material transferred between the friction pairs. Thus, adhesive wear manifested during the wear process. During adhesive wear, the materials transfer between pin and disk, like a soft aluminum matrix, adhere to the hard steel disk.

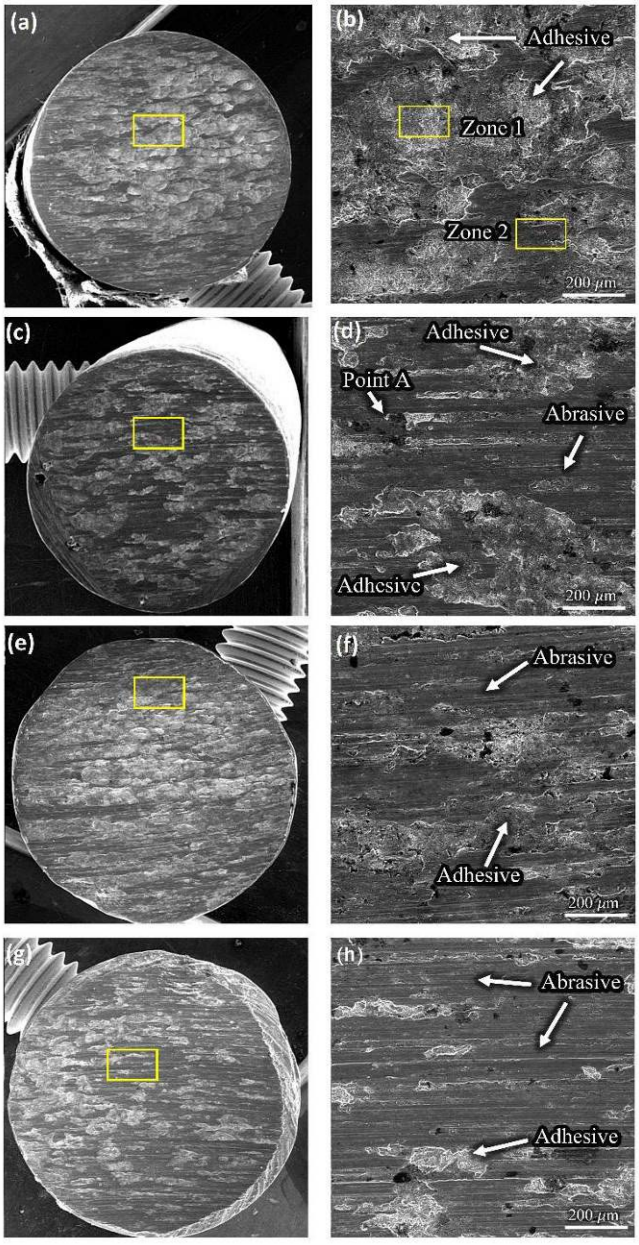

Fig. 12. The worn surfaces of hybrid composites: (a,b) A356/Al_2O_3+ZrO_2, (c,d) A356+Bi/Al_2O_3+ZrO_2, (e,f) A356+Sn/Al_2O_3+ZrO_2, and (g,h) A356+Bi/Al_2O_3+ZrO_2+SiC

Fig. 12c and 12d display the worn surface of the A356+Bi/Al_2O_3+ZrO_2 hybrid composite. It can be seen that the adhesive region decreased, and several parallel scratches indicating abrasive wear were observed. The EDS of point A is shown in Fig.13c, confirming the presence of Bi in the worn surface during sliding. It can typically occur when the lubricating role of Bi comes into play during sliding movements. Self-lubricating of Bi can minimize the sticking together of surfaces in contact, thus decreasing the occurrence of tiny connections formed due to the bonding of rough areas on the interacting

surfaces. This fact shows that the composite's wear mechanism depends on the microstructure constituent [41].

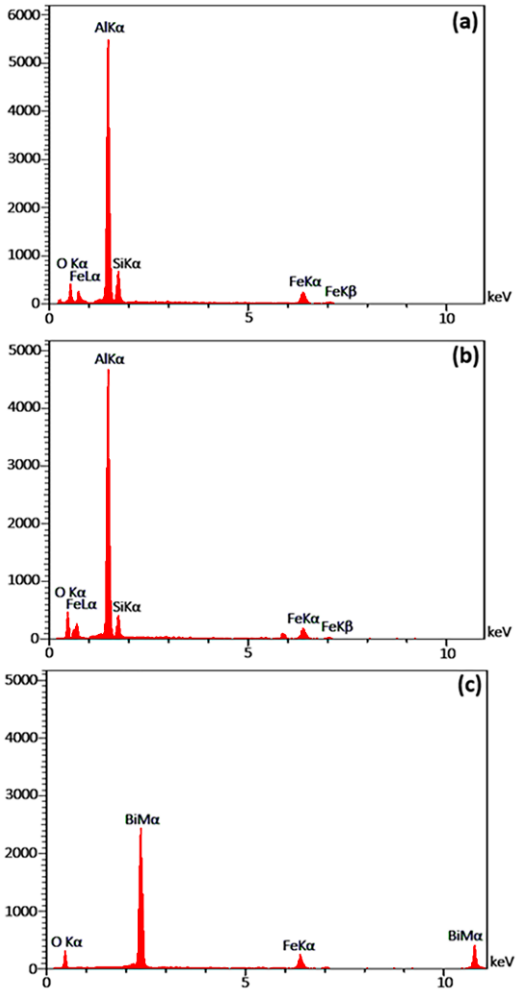

Fig. 13. Analysis of chemical elements of worn surface in (a) Zone 1 and (b) Zone 2 in Fig. 12b and (c) Point 3 in Fig. 12d

The worn surfaces of the A356+Sn/Al_2O_3+ZrO_2 hybrid composite are presented in Fig. 12e and 12f, with delamination and scratches detected on the wear test sample. Fig. 12g and 12h exhibit the worn surfaces of the A356+Bi/Al_2O_3+ZrO_2+SiC hybrid composite. It demonstrates the grooves that occur parallel to the sliding direction. The creation of parallel tracks on the pin surface indicates a shift in the wear mechanism from adhesive to the combination of abrasive and adhesive mode. Adhesive wear generally has a higher friction coefficient than abrasive wear. Adhesive wear is caused by transferring material from one surface to another due to forming a strong bond between the two surfaces, resulting in a higher FOC [42,43], as shown in Fig. 11.

On the other hand, abrasive wear is caused by hard particles or debris between two surfaces, resulting in a lower FOC [42]. It has been noted that abrasive wear is the only mechanism in which the wear characteristics directly correlate with the material's hardness. Hard particles can diminish the effective contact area between the friction pairs, thereby decreasing the material's removal. When subject to external force, the soft base tends to expose a significant portion of particles on the sample surface to bear the load. This was advantageous in preventing the direct involvement of the soft matrix in the friction process.

At the initiation of the wear process, adhesive wear takes precedence, predominantly resulting from the plastic deformation of the aluminum alloy matrix triggered by frictional heat, which leads to surface softening. The SWR experiences a substantial increase, as shown in Fig.10, accompanied by rapid escalation of the friction coefficient (Fig.11). However, after a specific duration, adhesive wear diminishes notably due to the emergence of fortified phase hard particles, ZrO_2, Al_2O_3, and SiC exposed on the matrix surface.

Subsequently, abrasive wear supersedes the primary wear mechanism, enhancing wear resistance to a certain extent (Figs. 12g and 12h). Simultaneously, Bi plays a pivotal role in lubrication and anti-friction by uniformly dispersing within the aluminum matrix. Therefore, the best tribological characteristics were obtained for A356+Bi/Al_2O_3+ZrO_2+SiC hybrid composite. Further research is imperative to accelerate our understanding of the impact of various weight proportions of ceramic particles on hybrid composites' mechanical and wear characteristics.

4. Conclusions

1. All Al_2O_3, ZrO_2, and SiC reinforcements were successfully incorporated inside the A356 matrix alloy via selective compo-casting route.
2. Both Bi and Sn elements were detected at the latter stage of solidification near the reinforcement particles, improving the interface's discontinuity and hybrid composite performance.
3. The lowest wear rate and friction coefficient were obtained for A356+Bi/ZrO_2+Al_2O_3+SiC hybrid composite under 5, 10, and 20 N applied loads.
4. Adhesive and abrasive mechanisms were detected in composite's worn surfaces. The composite sample demonstrating superior wear resistance exhibited a greater tendency towards abrasive wear and a lesser bias towards adhesive wear due to self-lubricating addition elements and integrating the harder reinforcement particle.
5. The lubricating role of Bi is more significant than Sn for reducing specific wear rates and friction coefficients in fabricated hybrid composites.

References

[1] Liang, Y.H., Wang, H.Y. & Yang, Y.F. (2008). Evolution process of the synthesis of TiC in the Cu-Ti-C system, *Journal of Allloys and Compounds*. 452(2), 298-303. https://doi.org/10.1016/j.jallcom.2006.11.024.

[2] Sahraeinejad, S., Izadi, H., Haghshenas, M. & Gerlich, A.P. (2015). Fabrication of metal matrix composites by friction stir processing with different Particles and processing parameters. *Materials Science and Engineering: A*. 626, 505-

513. https://doi.org/https://doi.org/10.1016/j.msea.2014.12.077.
[3] Devaraju, A., Kumar, A. & Kotiveerachari, B. (2013). Influence of addition of Grp/Al_2O_3p with SiCp on wear properties of aluminum alloy 6061-T6 hybrid composites via friction stir processing. *Transactions of Nonferrous Metals Society of China (English Edition)*. 23(5), 1275-1280. https://doi.org/10.1016/S1003-6326(13)62593-5.
[4] Rajmohan, T., Palanikumar, K. & Ranganathan, S. (2013). Evaluation of mechanical and wear properties of hybrid aluminium matrix composites. *Transactions of Nonferrous Metals Society of China (English Edition)*. 23(9), 2509-2517. https://doi.org/10.1016/S1003-6326(13)62762-4.
[5] Shayan, M., Eghbali, B. & Niroumand, B. (2019). Synthesis of AA2024-(SiO_2np+TiO_2np) hybrid nanocomposite via stir casting process. *Materials Science and Engineering A*. 756, 484-491. https://doi.org/10.1016/j.msea.2019.04.089.
[6] Rajmohan, T., Palanikumar, K. & Ranganathan, S. (2013). Evaluation of mechanical and wear properties of hybrid aluminium matrix composites. *Transactions of Nonferrous Metals Society of China.* 23(9), 2509-2517. https://doi.org/https://doi.org/10.1016/S1003-6326(13)62762-4.
[7] Lemine, A.S., Fayyaz, O., Yusuf, M., Shakoor, R.A., Ahmad, Z., Bhadra, J. & Al-Thani, N.J. (2022). Microstructure and mechanical properties of aluminum matrix composites with bimodal-sized hybrid NbC-B_4C reinforcements. *Materials Today Communications*. 33, 104512, 1-10. https://doi.org/https://doi.org/10.1016/j.mtcomm.2022.104512.
[8] Singh, J. & Chauhan, A. (2016). Characterization of hybrid aluminum matrix composites for advanced applications - A review. *Journal of Materials Research and Technology*. 5(2), 159-169. https://doi.org/10.1016/j.jmrt.2015.05.004.
[9] Fanani, E.W.A., Surojo, E., Prabowo, A.R. & Akbar, H.I. (2021). Recent progress in hybrid aluminum composite: Manufacturing and application, *Metals (Basel)*. 11(12), 1919, 1-30. https://doi.org/10.3390/met11121919.
[10] Chandel, R., Sharma, N. & Bansal, S.A. (2021). A review on recent developments of aluminum-based hybrid composites for automotive applications. *Emergent Materials*. 4, 1243-1257. https://doi.org/10.1007/s42247-021-00186-6.
[11] James, J.S., Ganesan, M., Santhamoorthy, P. & Kuppan, P. (2018). Development of hybrid aluminium metal matrix composite and study of property. *Materials Today Proceedings.* 5(5), 13048-13054. https://doi.org/https://doi.org/10.1016/j.matpr.2018.02.291.
[12] Srivyas, P.D. & Charoo, M.S. (2019). Application of hybrid aluminum matrix composite in automotive industry, in: *Materials Today Proceedings*. 18(7), 3189-3200. https://doi.org/10.1016/j.matpr.2019.07.195.
[13] Pranavi, U., Venkateshwar Reddy, P., Venukumar, S. & Cheepu, M. (2022). Evaluation of mechanical and wear properties of Al 5059/B_4C/Al_2O_3 hybrid metal matrix composites. *Journal of Composites Science*. 6(3), 86, 1-13. https://doi.org/10.3390/jcs6030086.
[14] Kumaran, S.T., Uthayakumar, M., Aravindan, S., Rajesh, S. (2016). Dry sliding wear behavior of SiC and B_4C-reinforced AA6351 metal matrix composite produced by stir casting process, Proceedings of the Institution of Mechanical Engineers, Part L: *Journal of Materials: Design and Applications*. 230(2), 484-491. https://doi.org/10.1177/1464420715579302.
[15] Khatkar, S.K., Suri, N.M., Kant, S. & Pankaj, (2018). A review on mechanical and tribological properties of graphite reinforced self lubricating hybrid metal matrix composites. *Reviews on Advanced Materials Science*. 56, 1-20. https://doi.org/10.1515/rams-2018-0036.
[16] Malaki, M., Fadaei Tehrani, A., Niroumand, B. & Gupta, M. (2021). Wettability in metal matrix composites. *Metals*. 11(7), 1034, 1-24. https://doi.org/10.3390/met11071034.
[17] Amirkhanlou, S. & Niroumand, B. (2010). Synthesis and characterization of 356-SiCp composites by stir casting and compocasting methods. *Transactions of Nonferrous Metals Society of China.* 20(3), 788-793. https://doi.org/https://doi.org/10.1016/S1003-6326(10)60582-1.
[18] Ghandvar, H., Farahany, S. & Idris, M.H. (2018). Effect of Wettability Enhancement of SiC Particles on Impact Toughness and Dry Sliding Wear Behavior of Compocasted A356/20SiCp Composites. *Tribology Transactions*. 61, 88-99. https://doi.org/10.1080/10402004.2016.1275902.
[19] Geng, L., Zhang, H., Li, H., Guan, L. & Huang, L. (2010). Effects of Mg content on microstructure and mechanical properties of SiCp/Al-Mg composites fabricated by semi-solid stirring technique. *Transactions of Nonferrous Metals Society of China* 20(10), 1851-1855. https://doi.org/https://doi.org/10.1016/S1003-6326(09)60385-X.
[20] Lashgari, H.R., Sufizadeh, A.R. & Emamy, M. (2010). The effect of strontium on the microstructure and wear properties of A356–10%B4C cast composites. *Materials & Design*. 31(4), 2187-2195. https://doi.org/10.1016/J.MATDES.2009.10.049.
[21] Sobczak, N. (2005). Effects of titanium on wettability and interfaces in aluminum/ceramic systems. In K. Ewsuk, K. Nogi, M. Reiterer, A. Tomsia, S. Jill Glass, R. Waesche, K. Uematsu & M. Naito (Eds.), *Characterization & Control of Interfaces for High Quality Advanced Materials* (81-91). OH, USA 83: The American Ceramic Society: Columbus.
[22] Wójcik-Grzybek, D., Frydman, K., Sobczak, N., Nowak, R., Piatkowska, A. & Pietrzak, K. (2017). Effect of Ti and Zr additions on wettability and work of adhesion in Ag/c system. *ElectronicMaterials*. 45(1), 4-11.
[23] Cao, C., Chen, L., Xu, J., Choi, H. & Li, X. (2016). Strengthening Al–Bi–TiC0.7N0.3 nanocomposites by Cu addition and grain refinement. *Materials Science and Engineering: A*. 651, 332-335. https://doi.org/https://doi.org/10.1016/j.msea.2015.10.126.
[24] Tao, Z., Guo, Q., Gao, X. & Liu, L. (2011). The wettability and interface thermal resistance of copper/graphite system with an addition of chromium. *Materials Chemistry and Physics*. 128(1-2), 228-232. https://doi.org/https://doi.org/10.1016/j.matchemphys.2011.03.003.
[25] Dasch, J.M., Ang, C.C., Wong, C.A., Waldo, R.A., Chester, D., Cheng, Y.T., Powell, B.R., Weiner, A.M. & Konca, E. (2009). The effect of free-machining elements on dry machining of B319 aluminum alloy. *Journal of Materials*

Processing Technology. 209(10), 4638-4644. https://doi.org/10.1016/j.jmatprotec.2008.11.041.
[26] Farahany, S., Ghandvar, H., Nordin, N.A., Ourdjini, A. & Idris, M.H. (2016). Effect of primary and eutectic Mg_2Si crystal modifications on the mechanical properties and sliding wear behaviour of an Al–20Mg_2Si–2Cu–xBi composite. *Journal of Materials Science & Technology*. 32(11), 1083-1097. https://doi.org/10.1016/j.jmst.2016.01.014.
[27] Ghandvar, H., Farahany, S. & Abu Bakar, T.A. (2020). A novel method to enhance the performance of an ex-situ Al/Si-YSZ metal matrix composite. *Journal of Alloys and Compounds.* 823, 153673, 1-14. https://doi.org/10.1016/J.JALLCOM.2020.153673.
[28] Barzani, M.M., Farahany, S., Yusof, N.M. & Ourdjini, A. (2013). The influence of bismuth, antimony, and strontium on microstructure, thermal, and machinability of aluminum-silicon alloy. *Materials and Manufacturing Processes*. 28(11), 1184-1190. https://doi.org/10.1080/10426914.2013.792425.
[29] Yusof, N.M., Razavykia, A., Farahany, S. & Esmaeilzadeh, A. (2016). Effect of modifier elements on machinability of Al-20%Mg2Si metal matrix composite during dry turning. *Machining Science and Technology*. 20(3), 460-474. https://doi.org/10.1080/10910344.2016.1191030.
[30] Mohanavel, V., Rajan, K., Suresh Kumar, S., Vijayan, G. & Vijayanand, M.S. (2018). Study on mechanical properties of graphite particulates reinforced aluminium matrix composite fabricated by stir casting technique. *Materials Today Proceedings*. 5(1), 2945-2950. https://doi.org/10.1016/j.matpr.2018.01.090.
[31] Sharma, P., Sharma, S. & Khanduja, D. (2016). Effect of graphite reinforcement on physical and mechanical properties of aluminum metal matrix composites. *Particulate Science and Technology*. 34 (1), 17-22. https://doi.org/10.1080/02726351.2015.1031924.
[32] Chandrasheker, J. Raju, N.V.S. (2022). Effect of Graphite Reinforcement on AA7050/B4C Metal Matrix Composites. *AIP Conference Proceedings*. 2648(1), 030013. https://doi.org/10.1063/5.0117657.
[33] Farahany, S., Ourdjini, A., Bakar, T.A.A. & Idris, M.H. (2014). On the refinement mechanism of silicon in Al-Si-Cu-Zn alloy with addition of bismuth. *Metallurgical and Materials Transactions A.* 45, 1085–1088. https://doi.org/10.1007/s11661-013-2158-0.
[34] Hemanth, J. (2005). Tribological behavior of cryogenically treated B4Cp/Al–12% Si composites. *Wear*. 258, 1732–1744. https://doi.org/10.1016/J.WEAR.2004.12.009.
[35] Uvaraja, V.C. & Natarajan, N. (2012). Optimization of Friction and Wear Behaviour in Hybrid Metal Matrix Composites Using Taguchi Technique. *Journal of Minerals and Materials Characterization and Engineering*. 11, 757-768. https://doi.org/10.4236/jmmce.2012.118063.
[36] Sharma, A., Sharma, V.M. & Paul, J. (2019). A comparative study on microstructural evolution and surface properties of graphene/CNT reinforced Al6061−SiC hybrid surface composite fabricated via friction stir processing. *Transactions of Nonferrous Metals Society of China (English Edition).* 29(10), 2005-2026. https://doi.org/10.1016/S1003-6326(19)65108-3.
[37] Amra, M., Ranjbar, K. & Hosseini, S.A. (2018). Microstructure and wear performance of Al5083/CeO_2/SiC mono and hybrid surface composites fabricated by friction stir processing. *Transactions of Nonferrous Metals Society of China (English Edition)*. 28(5), 866-878. https://doi.org/10.1016/S1003-6326(18)64720-X.
[38] Dinaharan, I. & Murugan, N. (2012). Dry sliding wear behavior of AA6061/ZrB 2 in-situ composite. *Transactions of Nonferrous Metals Society of China (English Edition)*. 22(4), 810-818. https://doi.org/10.1016/S1003-6326(11)61249-1.
[39] Riahi, A.R. & Alpas, A.T. (2001). The role of tribo-layers on the sliding wear behavior of graphitic aluminum matrix composites. *Wear*. 251 (1-12), 1396-1407. https://doi.org/10.1016/s0043-1648(01)00796-7.
[40] Archard, J.F. (1953). Contact and Rubbing of Flat Surfaces. *Journal of Applied Physics*. 24(8), 981–988. https://doi.org/10.1063/1.1721448.
[41] García, C., Martín, F., Herranz, G., Berges, C. & Romero, A. (2018). Effect of adding carbides on dry sliding wear behaviour of steel matrix composites processed by metal injection moulding, *Wear*. 414–415. https://doi.org/10.1016/j.wear.2018.08.010.
[42] Pei, X., Pu, W., Yang, J. & Zhang, Y. (2020). Friction and adhesive wear behavior caused by periodic impact in mixed-lubricated point contacts. *Advances in Mechanical Engineering*. 12(2). https://doi.org/10.1177/1687814020901666.
[43] Popova, E., Popov, V.L. & Kim, D.E. (2018). 60 years of Rabinowicz' criterion for adhesive wear. *Friction*. 6, 341-348. https://doi.org/10.1007/s40544-018-0240-8.